AD-A138 275 RESONANCE FLUORESCENCE OF A TWO-LEVEL ATOM NEAR A METAL SURFACE II CASE O..(U) ROCHESTER UNIV NY DEPT OF CHEMISTRY X Y HUANG ET AL. FEB 84 1/1

UNCLASSIFIED UROCHESTER/DC/84/TR-48 N00014-80-C-0427 F/G 7/4 NL

END

DATE FILMED

3-84

DTIC

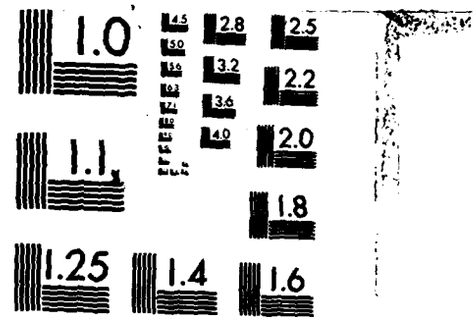

OFFICE OF NAVAL RESEARCH

Contract N00014-80-C-0472

Task No. NR 056-749

TECHNICAL REPORT No. 48

Resonance Fluorescence of a Two-Level Atom Near a Metal Surface. II. Case of a Strong Driving Field

by

Xi-Yi Huang and Thomas F. George

Prepared for Publication

in

Journal of Physical Chemistry

Department of Chemistry
University of Rochester
Rochester, New York 14627

February 1984

Unclassified

SECURITY CLASSIFICATION OF THIS PAGE (When Data Entered)

REPORT DOCUMENTATION PAGE		READ INSTRUCTIONS BEFORE COMPLETING FORM
1. REPORT NUMBER UROCHESTER/DC/84/TR-48	2. GOVT ACCESSION NO. AD-A138275	3. RECIPIENT'S CATALOG NUMBER
4. TITLE (and Subtitle) Resonance Fluorescence of a Two-Level Atom Near a Metal Surface. II. Case of a Strong Driving Field.		5. TYPE OF REPORT & PERIOD COVERED 6. PERFORMING ORG. REPORT NUMBER
7. AUTHOR(s) Xi-Yi Huang and Thomas F. George		8. CONTRACT OR GRANT NUMBER(s) N00014-80-C-0472
9. PERFORMING ORGANIZATION NAME AND ADDRESS Department of Chemistry University of Rochester Rochester, New York 14627		10. PROGRAM ELEMENT, PROJECT, TASK AREA & WORK UNIT NUMBERS NR 056-749
11. CONTROLLING OFFICE NAME AND ADDRESS Office of Naval Research Chemistry Program Code 472 Arlington, Virginia 22217		12. REPORT DATE February 1984 13. NUMBER OF PAGES 19
14. MONITORING AGENCY NAME & ADDRESS(if different from Controlling Office)		15. SECURITY CLASS. (of this report) Unclassified 15a. DECLASSIFICATION. DOWNGRADING SCHEDULE

16. DISTRIBUTION STATEMENT (of this Report)

This document has been approved for public release and sale; its distribution is unlimited.

17. DISTRIBUTION STATEMENT (of the abstract entered in Block 20, if different from Report)

18. SUPPLEMENTARY NOTES

Prepared for publication in the Journal of Physical Chemistry

19. KEY WORDS (Continue on reverse side if necessary and identify by block number)

RESONANCE FLUORESCENCE
TWO-LEVEL ATOM
METAL SURFACE
REFLECTED FIELD
PLASMON RESONANCE
SURFACE-DRESSED OPTICAL BLOCH EQUATIONS
STRONG DRIVING FIELD
THREE-PEAK FLUORESCENCE SPECTRUM
ASYMMETRY IN SIDE PEAKS

20. ABSTRACT (Continue on reverse side if necessary and identify by block number) The surface-dressed optical Bloch equations for a two-level atom near a metal surface are solved for the case of a strong driving field. An analytic form is obtained for the adatom resonance fluorescence spectrum. Due to the multiphoton effects of the surface-reflected field and the surface plasmon resonance, the three-peak spectrum is strongly influenced by the surface. A unique surface-induced asymmetry in the side peaks is revealed.

DD FORM 1 JAN 73 1473

Unclassified

SECURITY CLASSIFICATION OF THIS PAGE (When Data Entered)

Journal of Physical Chemistry, in press

RESONANCE FLUORESCENCE OF A TWO-LEVEL ATOM NEAR A METAL SURFACE. II. CASE OF A STRONG DRIVING FIELD

Xi-Yi Huang* and Thomas F. George
Department of Chemistry
University of Rochester
Rochester, New York 14627

ABSTRACT

The surface-dressed optical Bloch equations for a two-level atom near a metal surface are solved for the case of a strong driving field. An analytic form is obtained for the adatomic resonance fluorescence spectrum. Due to the multiphoton effects of the surface-reflected field and the surface plasmon resonance, the three-peak spectrum is strongly influenced by the surface. A unique surface-induced asymmetry in the side peaks is revealed.

*Permanent address: Institute of Physics, Academia Sinica, Beijing (Peking), The People's Republic of China

I. Introduction

In a recent paper[1] (which is paper I), we derived a set of surface-dressed optical Bloch equations, by which we discussed the effects of surface-reflected photons and a surface plasmon resonance on the weak-field resonance fluorescence spectrum. Our purpose in studying the surface-dressed optical Bloch equations is to investigate the basic behavior of the resonance excitation of a laser-driven quantum system near or adsorbed on a surface.[2-8] As a first step, we calculate the resonance fluorescence spectrum of a two-level atom near or adsorbed on a metal surface. At low laser intensity, if the excitation field is monochromatic, the atom absorbs a photon at the excitation frequency and the emitted photon has the same frequency, i.e., single-photon processes are dominant. The emitted radiation has the same spectral profile as the exciting radiation.

In the present paper, we extend the calculation to the case of a strong driving field, confining ourselves to the situation of a purely coherent laser field. In this case, many photons are involved in the adatom-surface resonant interaction, where nonlinear scattering can occur and multiphoton processes become as important as single-photon processes. This in turn leads to side bands emerging in the spectrum of the emitted radiation, and this so-called "dynamic Stark splitting" has attracted a great deal of interest recently. We are interested in the effects of the surface-reflected photons and surface plasmon resonance on these nonlinear multiphoton processes. In Section II the basic equations are presented, numerical results are shown in Section III, and concluding remarks are given in Section IV.

II. Basic Equations for a Two-Level Adatom

Consider a laser-driven two-level atom near or adsorbed on a metal surface. The field emitted by the induced atomic dipole will be reflected by the metallic surface, providing a surface-damped dynamic behavior of the adatom; the resonance interaction between the adatom and surface plasmon will further influence the light scattering spectrum of the adatom. The reflected field $\hat{E}_R(t)$ at the surface can be written as[1-3]

$$\hat{E}_R(t) = \mu_{12}\,\hat{\sigma}_{12}(t)\,f(d) + \mu_{21}\,\hat{\sigma}_{21}(t)\,f^*(d), \qquad (1)$$

where d is the distance between the adatom and surface, μ_{ij} is the electric-dipole transition matrix element between the adatomic states $|i\rangle$ and $|j\rangle$, $\hat{\sigma}_{ij} \equiv |i\rangle\langle j|$ is the adatomic transition operator, and f(d) is a distance-dependent function, which has been discussed in detail in 1. Knowing f(d), we can evaluate the surface-induced phase-decay constant, $\gamma_s \equiv (2/\hbar)\mathrm{Im}(f)|\mu_{12}|^2$. For the case of a laser-excited atom emitting near a metallic half-space, the imaginary part of f(d) has the following form:[1-4]

$$\mathrm{Im}(f) = \frac{\zeta}{1+\epsilon_1^2} \frac{k_1^3}{\left(\omega^2 - \frac{\omega_p^2}{1+\epsilon_1}\right)^2 + \frac{\delta^2\omega_p^4}{(1+\epsilon_1)^2\omega^2}}$$

$$\times \left\{ \frac{1}{\epsilon_1} \left[(\omega^2 - \omega_p^2)^2 + \frac{\omega_p^4\delta^2}{\omega^2} - \epsilon_1^2\omega^4 \right] \left[\eta \sin D - \frac{1}{D^2}\cos D \right] \right. \qquad (2)$$

$$\left. + 2\omega\delta\omega_p^2 \left[\eta \cos D + \frac{1}{D^2}\sin D \right] \right\} ,$$

where $\zeta = 1$ and $\eta \equiv 1/D^3 + 1/D$ for the case of the induced dipole oriented parallel to the surface, $\zeta = 2$ and $\eta \equiv 1/D^3$ for the perpendicular case, ϵ_1 is the dielectric constant for the gas medium, $k_1 = \omega\sqrt{\epsilon_1}/c$ is the wave number, ω is the emission frequency, and $D = 2k_1 d$ is the reduced distance which is dimensionless. The Drude model[9] has been used for the metal medium in eq. 2, and the metallic dielectric constant is

$$\epsilon_2(\omega) = 1 - \frac{\omega_p^2}{\omega(\omega+i\delta)} , \qquad (3)$$

where δ is the inverse of the relaxation time and ω_p is the plasma frequency. Im(f) has a resonance at $\omega_{sp} = \omega_p(1+\varepsilon_1)^{-1/2}$, which is the surface plasmon frequency of the interface.

Using eq. 2, we can express the surface-induced phase-decay constant [in the unit of Einstein's spontaneous decay coefficient $A \equiv 4\omega_{21}^3/(3\hbar c)|\mu_{21}|^2$] in the following form:

$$\gamma_s = \zeta\, a_0 \left[a_1\left(\eta \sin D - \frac{\cos D}{D^2}\right) + a_2\left(\eta \cos D + \frac{\sin D}{D^2}\right)\right] \tag{4}$$

where

$$a_0 = \frac{3}{8}\,\frac{1}{(1-\beta^2)^2 + (\alpha/\omega_{sp})^2} \tag{5}$$

$$a_1 = (2-\beta^2)^2 + (2\alpha/\omega_{sp})^2 - \beta^4 \tag{6}$$

$$a_2 = (2\beta)^2\, \alpha/\omega_{sp}\ , \tag{7}$$

$\beta \equiv \omega_L/\omega_{sp}$, $\alpha \equiv \delta/\beta$, and $\varepsilon_1 = 1$ has been assumed so that $\omega_{sp} = \omega_p/\sqrt{2}$.

Accounting for the surface-reflected photons and the surface plasmon resonance, the surface-dressed optical Bloch equations (SBE) take the form (within the rotating-wave approximation and the equilibrium condition $\hat{W}(0) = -1$)[1-3]

$$\frac{d}{dt}\begin{pmatrix} \hat{S}_{21}(t) \\ \hat{W}(t) \\ \hat{S}_{12}(t) \end{pmatrix} = \begin{pmatrix} -\tilde{\gamma}_2 + i\Delta & i\Omega/2 & 0 \\ i\Omega & -\gamma_1 & -i\Omega \\ 0 & -i\Omega/2 & -\tilde{\gamma}_2 - i\Delta \end{pmatrix} \times \begin{pmatrix} \hat{S}_{21}(t) \\ \hat{W}(t) \\ \hat{S}_{12}(t) \end{pmatrix} - \gamma_1 \begin{pmatrix} 0 \\ 1 \\ 0 \end{pmatrix} . \tag{8}$$

$\hat{S}_{12}(t) \equiv \hat{\sigma}_{12}(t)\exp(iW_L t)$, $\hat{S}_{21}(t) \equiv \hat{\sigma}_{21}(t)\exp(-iW_L t)$, the Rabi frequency is $\Omega \equiv (2/\hbar)\,|\mu_{21}|E$, E is the amplitude of the electric field strength operator in a coherent state[10] of the laser field with frequency ω_L, $\Delta \equiv \omega_{21} - \omega_L$ is the detuning, ω_{21} is the adatomic transition frequency, γ_1 is the population relaxation constant, γ_2 is the phase relaxation constant, $\tilde{\gamma}_2 \equiv \gamma_2 + \gamma_s$, and $\hat{W}(t) \equiv \hat{\sigma}_{22}(t) - \hat{\sigma}_{11}(t)$ is the population inversion of the adatom.

When the intensity of the coherent laser field is very large, $\Omega^2 + \Delta^2 >> \tilde{\gamma}_2^2$, the scattering light spectrum $S(\omega)$ of the adatom at steady state can be obtained as the Fourier transform the dipole-dipole correlation function $\langle \hat{S}_{21}(t_1)\, \hat{S}_{12}(t_2) \rangle$ in the following analytical form:

$$
\begin{aligned}
S(\omega) = \frac{\Omega^2}{\Delta^2 + \alpha\Omega^2} \Bigg[& \frac{\Delta^2 + \tilde{\gamma}_2}{\Delta^2 + \alpha\Omega^2}\, \delta(\omega - \omega_L) \\
& + \frac{\Omega^2[(2\alpha-1)\Delta^2 + \alpha^2\Omega^2]}{(\Delta^2 + \Omega^2)(\Delta^2 + \alpha\Omega^2)} \left(\frac{S_0/\pi}{(\omega-\omega_L)^2 + S_0^2} \right) \\
& + \frac{1}{2}\, \frac{(\Omega'-\Delta)[\alpha(\Omega'-\Delta) + \Delta]}{(\Delta^2 + \Omega^2)} \left(\frac{S_\pm/\pi}{(\omega-\omega_L+\Omega')^2 + S_\pm^2} \right) \\
& + \frac{1}{2}\, \frac{(\Omega'+\Delta)[\alpha(\Omega'+\Delta) - \Delta]}{(\Delta^2 + \Omega^2)} \left(\frac{S_\pm/\pi}{(\omega-\omega_L-\Omega')^2 + S_\pm^2} \right) \Bigg] .
\end{aligned}
\tag{9}
$$

The parameter α is defined as

$$\alpha \equiv \tilde{\gamma}_2/2\gamma_2 \tag{10}$$

the detuning parameter is defined as

$$\Omega' \equiv \Delta + \Delta_s, \tag{11}$$

where

$$\Delta_s = \Delta\{[1 + (\Omega/\Delta)^2]^{\frac{1}{2}} - 1\}, \tag{12}$$

and the widths of the profiles are

$$S_o = 2\gamma_2 \left(\frac{\alpha\Omega^2 + \Delta^2}{\Omega^2 + \Delta^2}\right) \tag{13a}$$

$$S_\pm = S_+ = S_- = \gamma_2 \left(\frac{(1+\alpha)\Omega^2 + 2\alpha\Delta^2}{\Omega^2 + \Delta^2}\right). \tag{13b}$$

There are four components in the emission spectrum given by eq. 9. The first two terms are centered at the frequency ω_L of the driving laser. These terms are identified as the coherent and incoherent parts of the Rayleigh scattering. The incoherent Rayleigh component is unimportant at low laser intensity but becomes dominent at high laser intensity. The third and fourth terms are centered at $\omega_3 = \omega_L-(\Delta+\Delta_s)$ and $\omega_F = \omega_L+(\Delta+\Delta_s)$. These "side bands" are due to higher-order photon interactions. The processes leading to the side bands can be explained by Figure 1. With the laser detuning $\Delta=\omega_{21}-\omega_L\neq 0$, two laser photons are absorbed and a photon is emitted to produce an excited state of the adatom. This "three-photon" component is given by the third term of eq. 9, which has a maximum at ω_3. Since an excited state is produced for every photon generated at ω_3, there will also be emission at $\omega_F=\omega_{21}+\Delta_s$ from the excited atom (Figure 1a). A single-photon process with the aid of surface damping can also overcome the gap between ω_L and ω_{21} to give rise to fluorescence at ω_F (Figure 1b). Such a process affects the strength of the coherent Rayleigh scattering, as well as broadening and altering the heights of the spectral components of the incoherent Rayleigh scattering, "three-photon" scattering and fluorescence.

When $\Omega^2 + \Delta^2 >> \tilde{\gamma}_2^2$, the three peaks can be resolved, whose integrated intensities are:

$$I_R = \left(\frac{W_L}{\omega_0}\right)^3 \frac{(\gamma_2/2)\,\Omega^2}{\Delta^2} \tag{14}$$

$$I_3 = \frac{(\gamma_2/4)\Omega^2(\Omega'-\Delta)[\alpha(\Omega'-\Delta)+\Delta]}{(\Delta^2+\Omega^2)(\Delta^2+\alpha\Omega^2)} \tag{15}$$

$$I_F = \frac{(\gamma_2/4)\Omega^2(\Omega'+\Delta)[\alpha(\Omega'+\Delta)-\Delta]}{(\Delta^2+\Omega^2)(\Delta^2+\eta\Omega^2)} \quad , \tag{16}$$

where I_R, I_3 and I_F are the intensities for Raman scattering, three-photon scattering and fluorescence, respectively. From eqs. 14-16, we see that I_R is unaffected by the surface damping, but I_3 and I_F can be influenced by the surface through the parameter α.

We can also see from eq. 9 that the condition of "weak excitation", corresponding to the weak-field limit, can be precisely stated as

$$\alpha\,\Omega^2 \ll \Delta^2 \quad . \tag{17}$$

In this case, where the laser is "weak" and the surface damping rates are low, the spectrum given by eq. 9 reduces to the low-intensity limit given by eq. 19 of paper I(for $\gamma_L \to 0$).[1]

III. Numerical Results

Using the strong-field formula of eq. 9 for the case of a two-level atom near or adsorbed on a metal surface, we have evaluated numerically the surface-modified resonance fluorescence spectrum. A sample spectrum is shown in Figure 2, where we see the Rayleigh (central) peak, the three-photon peak (left) and the fluorescence peak (right). In this picture we have drawn just the profile of the incoherent component of the Rayleigh scattering, as the coherent component is not broadened by the surface. The adatom has a resonant interaction with

the surface plasmon, i.e., $\beta=\omega_L/\omega_{sp}=1$. We have used the value of 3.5×10^{-3} for the ratio δ/ω_{sp}, which corresponds to a silver surface.

To interpret the spectrum, we first review the surface-free situation, i.e., when the adatom-surface distance is very large ($D\to\infty$). In this case the three-peak spectrum is symmetric, where the two side peaks have the same height (intensity). The reason for this is the following: Two laser photons of frequency $\omega_L \mp \omega_{21}$ are absorbed, a photon is emitted at ω_3, and an excited state produced (Figure 1a); since an excited state is produced for every photon generated at ω_3, there is also emission at $\omega_F=\omega_{21}+\Delta_s$ from the excited state, and hence the two side peaks have equal intensity. When the adatom-surface distance becomes smaller, such as D=2 in Figure 2, the symmetry of the spectrum is destroyed. This results from an "interference" between the incident laser field and the reflected field from the surface,[1-3] whereby the peaks are altered and broadened by the surface. This becomes more dramatic as the detuning increases, as shown in Figure 3 for the large-detuning case $\Delta=\Omega=10$ (in the unit of Einstein's A-coefficient). We also note that the spectrum is more influenced by the surface when the transition dipole is oriented parallel to the surface rather than perpendicular.

In the case of a gas-phase collision-modified process, the random collision interruption causes the fluorescence peak to be higher than the "three-photon" peak (for positive detuning).[11] Such asymmetry has been observed experimentally.[12] However, for the surface-damped process this does not always occur, due to the interference between the coherence incident and reflected fields which leads to an oscillatory distance dependence of the emission intensity. This is displayed in Figures 4 and 5. While the height H_+ and integrated power P_+ of the fluorescence component (P_+ is the area under the curve for the fluorescence component) are generally larger than those of the three-photon components, H_- and P_-, the reverse occurs for some adatom-surface distances. This is a unique behavior at a surface which has not been predicted for the usual gas-phase atomic collision case.

We would now like to propose an experimental scheme to test our theoretical results. Figure 6 shows an arrangement for such testing on a metal substrate (gold, silver or copper), where a number of layers of fatty acid are placed by the Langmuir-Blodgett dipping technique,[13] and a thin layer of sodium atoms is then put on the top of this assembly. In this way, the sodium atoms are at a known fixed distance d from the metal. These atoms are then excited by a laser beam propagating parallel to the metal surface, whose polarization can be adjusted to be parallel or perpendicular to the surface. To avoid interaction among the sodium atoms, a low density ($\sim 10^{12}/cm^3$) of sodium deposited in a thin layer is required. The laser-induced flurescence from the $3P_{3/2}(F'=3) \rightarrow 2S_{1/2}(F=2)$ transition of Na is analyzed by a Fabry-Perot interferometer along the normal direction of the metal surface. This particular atomic transition is chosen because it is a two-level transition and the atomic population cannot be optically pumped into a third level.[14] The dye laser produces 1 - 100 cm^2 of peak intensities at 5890 Å. The light transmitted through the Fabry-Perot interferometer is detected by a cooled photomultiplier, followed by photon-counting electronics. A two-peak spectrum in weak excitation ($\sim 1 W/cm^2$) and a three-peak spectrum in strong excitation ($\sim 100\ W/cm^2$) should be observable, using different values of laser intensities, detunings, adatom-surface separations and surface plasmon resonance conditions.

IV. Concluding Remarks

In this work, we have solved the surface-dressed optical Bloch equations for the case of a strong driving field. An analytic form is obtained for the two-level adatomic resonance fluorescence spectrum. It is shown that the surface-reflected field and surface plasmon resonance will strongly modify the spectrum. Due to the interference between the incident laser field and the surface-reflected field, an interesting surface-induced asymmetry occurs in the side bands which is quite different from the usual gas-phase collision-induced asymmetry.

Surface-enhanced photochemistry is an interesting phenomenon,[15,16] and we are looking at extensions of our model to other types of spectroscopic and dynamic problems. These include the cooperative spectroscopy of many interacting atoms near a surface and the excitation and dissociation processes of polyatomic molecules adsorbed on a metallic surface, taking into account surface roughness.

Acknowledgements

This work was supported in part by the Air Force Office of Scientific Research (AFSC), United States Air Force, under Grant AFOSR-82-0046, the Office of Naval Research and the U.S. Army Research Office. The United States Government is authorized to reproduce and distribute reprints for governmental purposes notwithstanding any copyright notation hereon. TFG acknowledges the Camille and Henry Dreyfus Foundation for a Teacher-Scholar Award (1975-84) and the John Simon Guggenheim Memorial Foundation for a Fellowship (1983-84). XYH thanks Prof. M. G. Raymer for a useful discussion.

REFERENCES

1. X. Y. Huang, J. Lin and T. F. George, J. Chem. Phys., 80, 893 (1984).
2. X. Y. Huang, J. Lin and T. F. George in Coherence and Quantum Optics V, ed. by L. Mandel and E. Wolf (Plenum, New York), in press.
3. J. Lin, X. Y. Huang and T. F. George, Solid State Commun., 47, 63 (1983).
4. See the review by R. R. Chance, A. Prock, and R. Silbey, Adv. Chem. Phys., 37, 1 (1978).
5. See the review article by T. E. Furtak and J. Reyes, Surf. Sci., 93, 351 (1980).
6. A. M. Glass, P. F. Liao, J. G. Bergman and D. H. Olson, Opt. Lett., 5, 368 (1980).
7. J. F. Owen, P. W. Barber, P. B. Dorain and R. K. Chang, Phys. Rev. Lett., 47, 1075 (1981).
8. D. A. Wetz, S. Garoff, J. I. Gersten and A. Nitzan, J. Chem. Phys., 78, 5324 (1983).

9. M. Born and W. Wolf, Principles of Optics (Pergamon, New York, 1975), pp. 624-627.

10. R. J. Glauber in Quantum Optics and Electronics, ed. by C. Dewitt, A. Blandin and C. Cohen-Tannoudji (Gordon and Breach, New York, 1965), pp. 65-185.

11. B. R. Mollow, Phys. Rev. A, 15, 1023 (1977).

12. J. L. Carlsten, A. Szöke and M. G. Raymer, Phys. Rev. A, 15, 1029 (1977).

13. H. Kuhn, J. Chem. Phys. 53, 101 (1970).

14. F. Schuda, C. R. Stroud, Jr. and M. Hercher, J. Phys. B: Atom. Molec. Phys., 7, L198 (1974).

15. A. Nitzan and L. E. Brus, J. Chem. Phys. 74, 537 (1981); 75, 2205 (1981).

16. C. J. Chen and R. M. Osgood, Phys. Rev. Lett., 50, 1705 (1983).

FIGURE CAPTIONS

Figure 1. Basic processes for the three-photon and fluorescence components of the spectrum: (a) Three-photon scattering at $\omega_3=2\omega_L-(\omega_{21}+\Delta_s)$ and consequent fluorescence at $\omega_{21}+\Delta_s$, where the adatomic levels are separated by the transition frequency ω_{21} plus the laser-induced level shift Δ_s; (b) fluorescence at $\omega_{21}+\Delta_s$ induced by surface coupling.

Figure 2. Strong-field surface-modified resonance fluorescence spectrum, including just the incoherent component of Rayleigh scattering, for $(\Delta,\Omega,\beta)=(1,10,1)$, where Δ and Ω are in the unit of A. Curve 1 corresponds to a very large value of the reduced distance, i.e. $D=2k_1d\to\infty$, which is the surface-free case where the spectrum is symmetric, while curves 2 (solid) and 2' (dashed) correspond to the value of the reduced distance D=2, where the symmetry is broken. The solid curve is for the induced transition dipole oriented perpendicular to the surface, and the dashed curve is for the parallel case. X denotes $(\omega-\omega_L)/\Omega'$ on the horizontal axis.

Figure 3. Strong-field surface-modified resonance fluorescence spectrum, including just the incoherent component of Rayleigh scattering, for $(\Delta,\Omega,\beta)=(10,10,1)$. The labelling is the same as in Figure 2.

Figure 4. Adatom-surface distance dependence of the heights of the three peaks in the resonance fluorescence spectrum for (Δ,Ω,β) (1,10,1). H_-, H_0 and H_+ correspond to the peak heights of the three-photon, incoherent Rayleigh and fluorescence components, respectively. The solid curves are for the induced transition dipole oriented perpendicular to the surface, and the dashed curves are for the parallel case.

Figure 5. Distance dependence of the integrated power of the three peaks in the resonance fluorescence spectrum, where P_-, P_0 and P_+ correspond the integrated powers of the three-photon, Rayleigh and fluorescence peaks, respectively. The labelling is the same as in Figure 4.

Figure 6. Proposed experiment for testing the theoretical results.

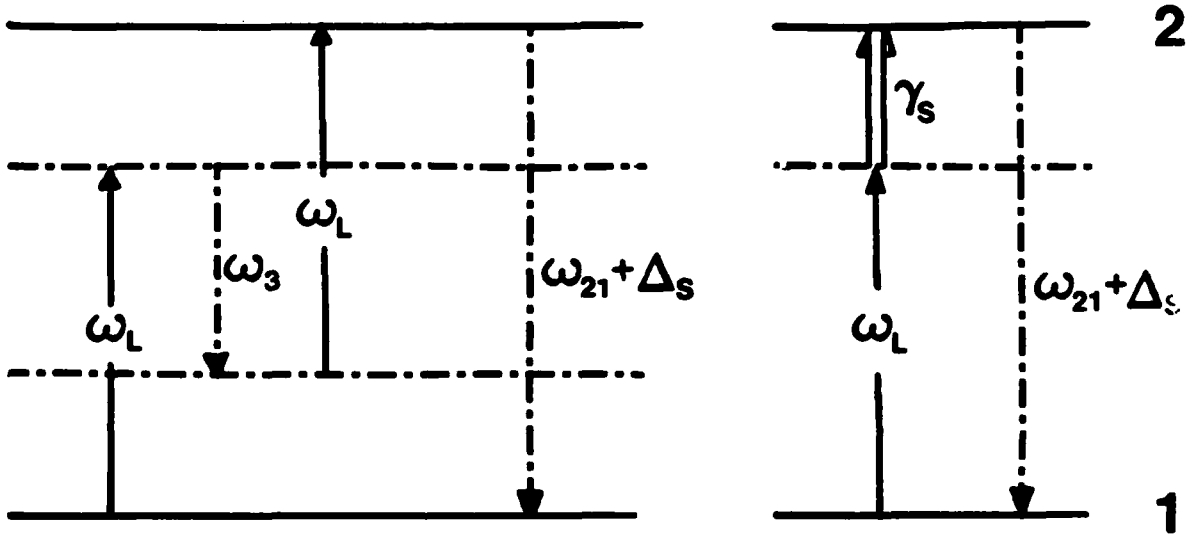
2
1
ω_L
ω_3
ω_L
$\omega_{21}+\Delta_S$
γ_S
ω_L
$\omega_{21}+\Delta_S$
a
b

Fig. 1

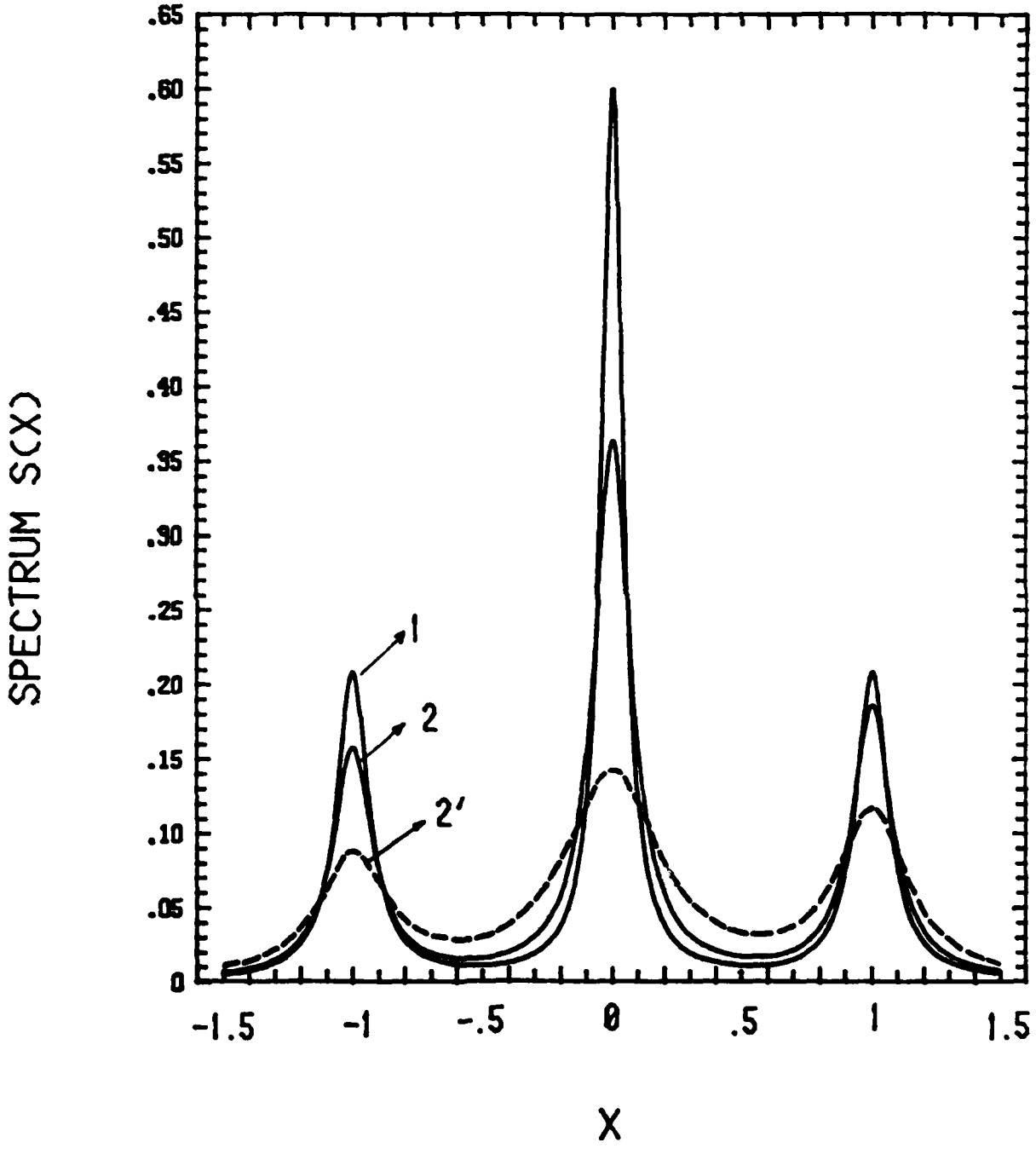
SPECTRUM S(X)
.65
.60
.55
.50
.45
.40
.35
.30
.25
.20
.15
.10
.05
0
-1.5
-1
-.5
0
.5
1
1.5
X
1
2
2'

Fig. 2

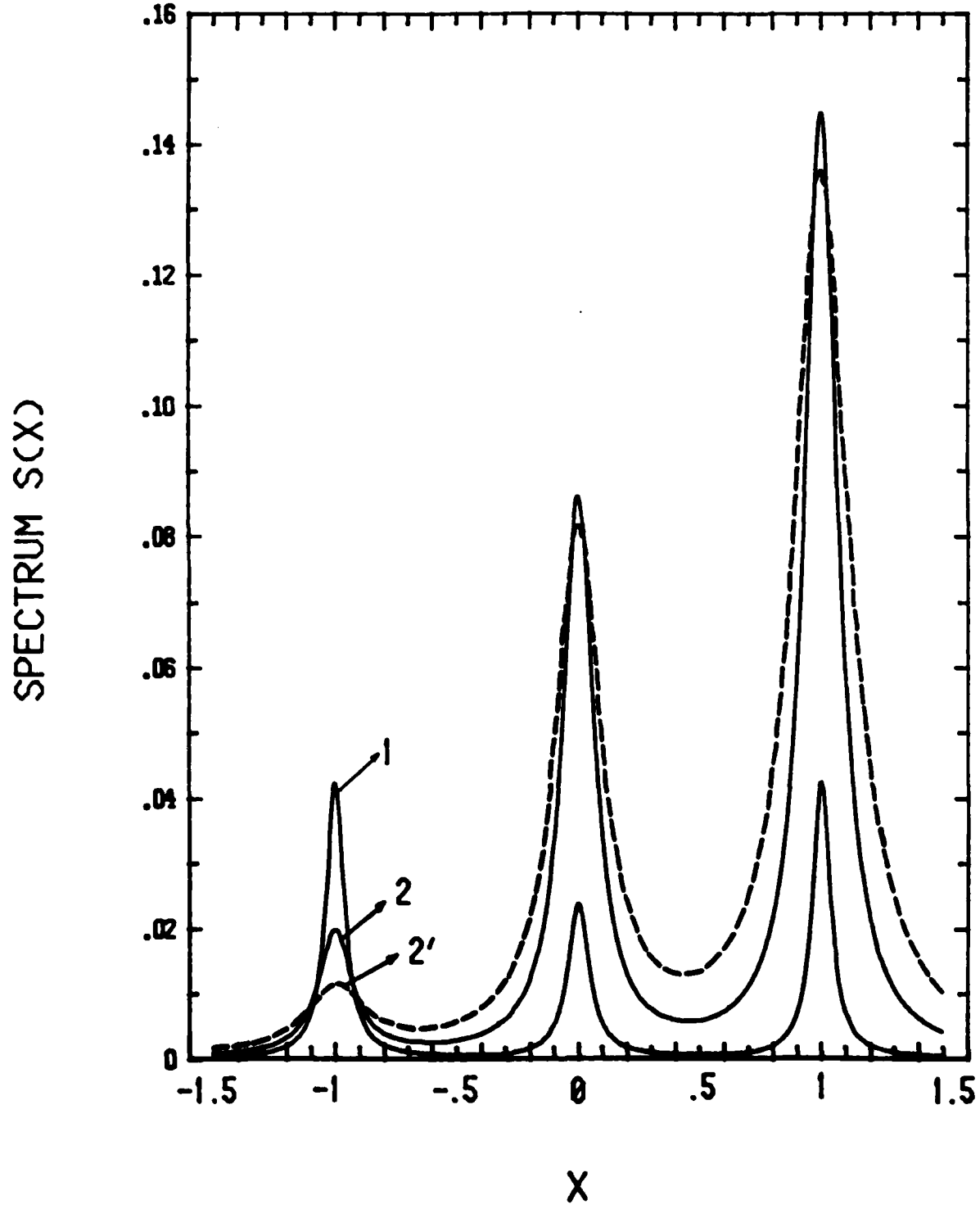

Fig. 3

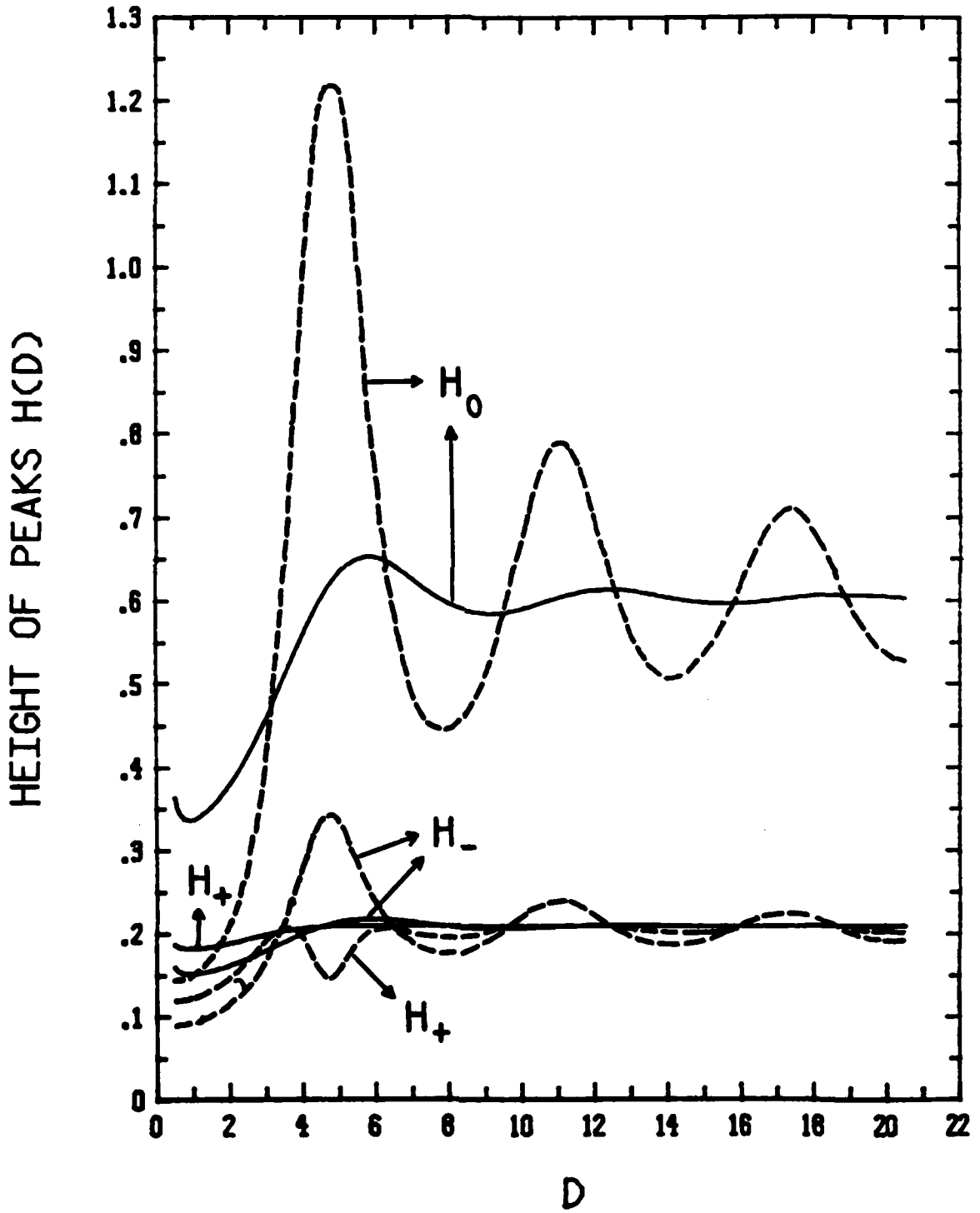
HEIGHT OF PEAKS H(D)
1.3
1.2
1.1
1.0
.9
.8
.7
.6
.5
.4
.3
.2
.1
0
0
2
4
6
8
10
12
14
16
18
20
22
D
H_0
H_-
H_+
H_+

Fig. 4

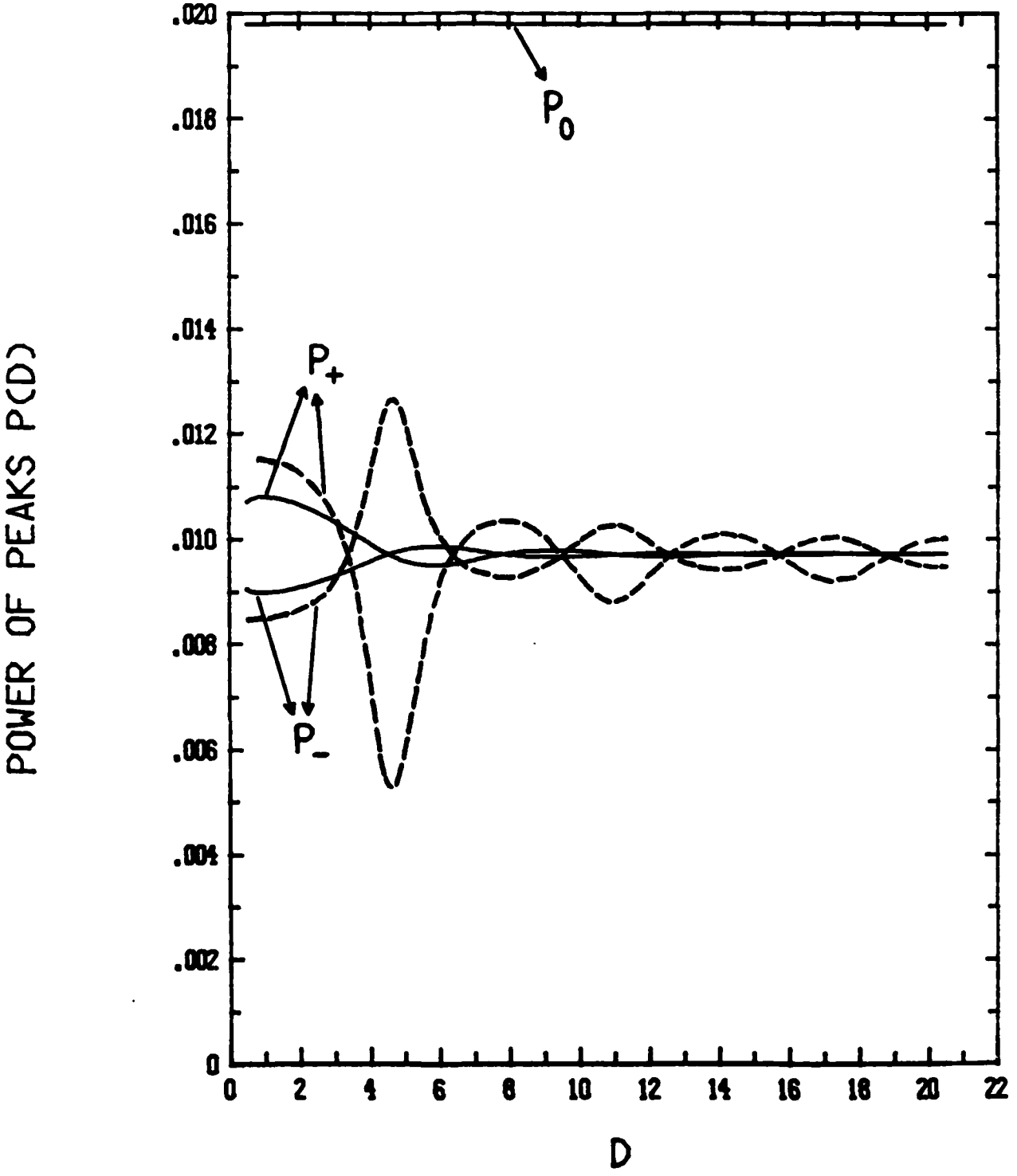
POWER OF PEAKS P(D)
.020
.018
.016
.014
.012
.010
.008
.006
.004
.002
0
P_0
P_+
P_-
0
2
4
6
8
10
12
14
16
18
20
22
D

Fig. 5

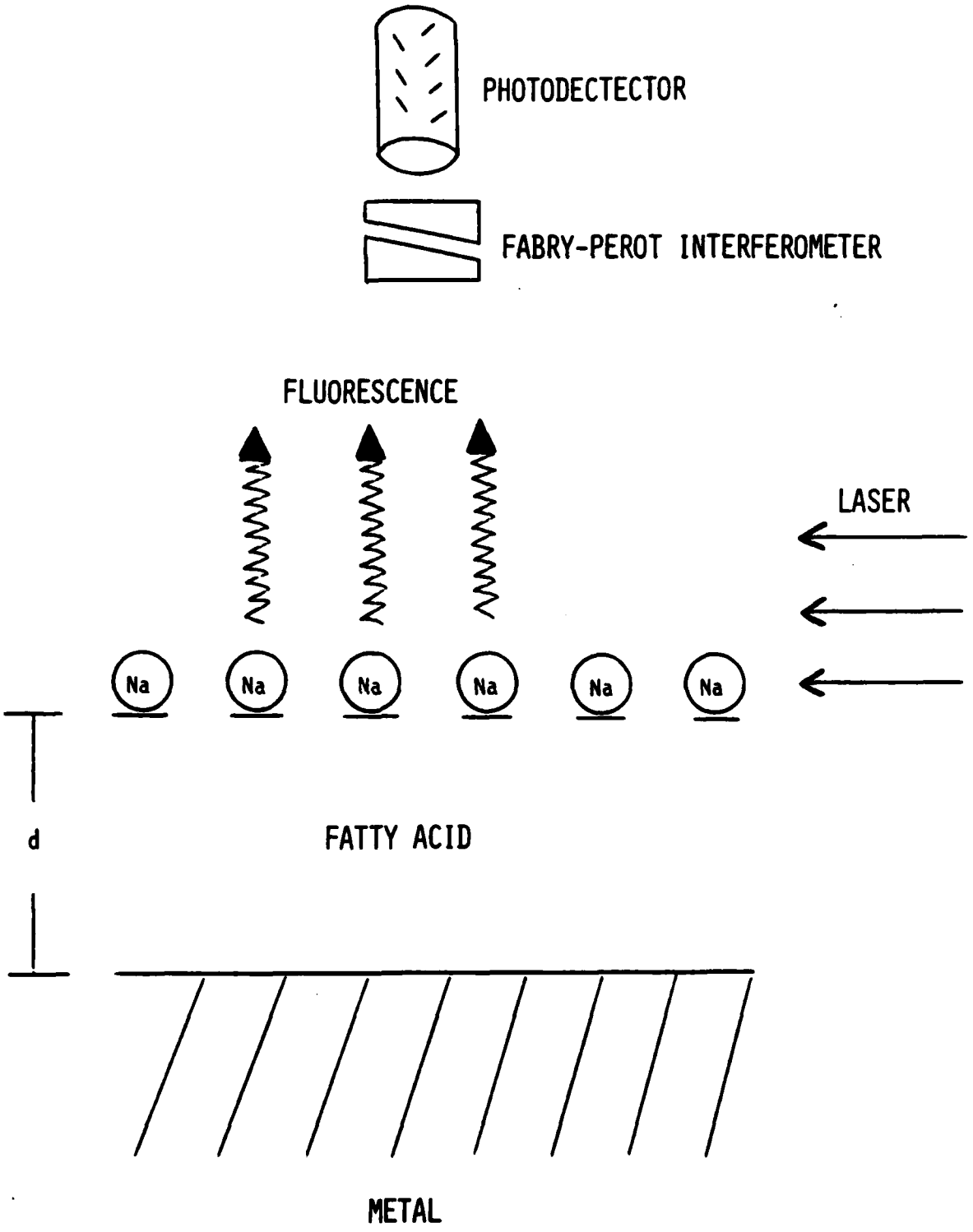
PHOTODECTECTOR
FABRY-PEROT INTERFEROMETER
FLUORESCENCE
LASER
Na
Na
Na
Na
Na
Na
d
FATTY ACID
METAL

Fig. 6

DL/413/83/01
GEN/413-2

TECHNICAL REPORT DISTRIBUTION LIST, GEN

	No. Copies
Office of Naval Research Attn: Code 413 800 N. Quincy Street Arlington, Virginia 22217	2
ONR Pasadena Detachment Attn: Dr. R. J. Marcus 1030 East Green Street Pasadena, California 91106	1
Commander, Naval Air Systems Command Attn: Code 310C (H. Rosenwasser) Washington, D.C. 20360	1
Naval Civil Engineering Laboratory Attn: Dr. R. W. Drisko Port Hueneme, California 93401	1
Superintendent Chemistry Division, Code 6100 Naval Research Laboratory Washington, D.C. 20375	1
Defense Technical Information Center Building 5, Cameron Station Alexandria, Virginia 22314	12
DTNSRDC Attn: Dr. G. Bosmajian Applied Chemistry Division Annapolis, Maryland 21401	1
Naval Ocean Systems Center Attn: Dr. S. Yamamoto Marine Sciences Division San Diego, California 91232	1
Dr. David L. Nelson Chemistry Program Office of Naval Research 800 North Quincy Street Arlington, Virginia 22217	1
Naval Ocean Systems Center Attn: Technical Library San Diego, California 92152	1
Naval Weapons Center Attn: Dr. A. B. Amster Chemistry Division China Lake, California 93555	1
Scientific Advisor Commandant of the Marine Corps Code RD-1 Washington, D.C. 20380	1
Dean William Tolles Naval Postgraduate School Monterey, California 93940	1
U.S. Army Research Office Attn: CRD-AA-IP P.O. Box 12211 Research Triangle Park, NC 27709	1
Mr. Vincent Schaper DTNSRDC Code 2830 Annapolis, Maryland 21402	1
Mr. John Boyle Materials Branch Naval Ship Engineering Center Philadelphia, Pennsylvania 19112	1
Mr. A. M. Anzalone Administrative Librarian PLASTEC/ARRADCOM Bldg 3401 Dover, New Jersey 07801	1

DL/413/83/01
056/413-2

TECHNICAL REPORT DISTRIBUTION LIST, 056

Dr. G. A. Somorjai
Department of Chemistry
University of California
Berkeley, California 94720

Dr. J. Murday
Naval Research Laboratory
Surface Chemistry Division (6170)
455 Overlook Avenue, S.W.
Washington, D.C. 20375

Dr. J. B. Hudson
Materials Division
Rensselaer Polytechnic Institute
Troy, New York 12181

Dr. Theodore E. Madey
Surface Chemistry Section
Department of Commerce
National Bureau of Standards
Washington, D.C. 20234

Dr. Chia-wei Woo
Department of Physics
Northwestern University
Evanston, Illinois 60201

Dr. Robert M. Hexter
Department of Chemistry
University of Minnesota
Minneapolis, Minnesota

Dr. J. E. Demuth
IBM Corporation
Thomas J. Watson Research Center
P.O. Box 218
Yorktown Heights, New York 10598

Dr. M. G. Lagally
Department of Metallurgical
and Mining Engineering
University of Wisconsin
Madison, Wisconsin 53706

Dr. Adolph B. Amster
Chemistry Division
Naval Weapons Center
China Lake, California 93555

Dr. W. Kohn
Department of Physics
University of California, San Diego
La Jolla, California 92037

Dr. R. L. Park
Director, Center of Materials
Research
University of Maryland
College Park, Maryland 20742

Dr. W. T. Peria
Electrical Engineering Department
University of Minnesota
Minneapolis, Minnesota 55455

Dr. Keith H. Johnson
Department of Metallurgy and
Materials Science
Massachusetts Institute of Technology
Cambridge, Massachusetts 02139

Dr. J. M. White
Department of Chemistry
University of Texas
Austin, Texas 78712

Dr. R. P. Van Duyne
Chemistry Department
Northwestern University
Evanston, Illinois 60201

Dr. S. Sibener
Department of Chemistry
James Franck Institute
5640 Ellis Avenue
Chicago, Illinois 60637

Dr. Arold Green
Quantum Surface Dynamics Branch
Code 3817
Naval Weapons Center
China Lake, California 93555

Dr. S. L. Bernasek
Princeton University
Department of Chemistry
Princeton, New Jersey 08544

DL/413/83/01
056/413-2

TECHNICAL REPORT DISTRIBUTION LIST, 056

Dr. F. Carter
Code 6132
Naval Research Laboratory
Washington, D.C. 20375

Dr. Richard Colton
Code 6112
Naval Research Laboratory
Washington, D.C. 20375

Dr. Dan Pierce
National Bureau of Standards
Optical Physics Division
Washington, D.C. 20234

Professor R. Stanley Williams
Department of Chemistry
University of California
Los Angeles, California 90024

Dr. R. P. Messmer
Materials Characterization Lab.
General Electric Company
Schenectady, New York ~~22217~~ 12301

Dr. Robert Gomer
Department of Chemistry
James Franck Institute
5640 Ellis Avenue
Chicago, Illinois 60637

Dr. Ronald Lee
R301
Naval Surface Weapons Center
White Oak
Silver Spring, Maryland 20910

Dr. Paul Schoen
Code 5570
Naval Research Laboratory
Washington, D.C. 20375

Dr. John T. Yates
Department of Chemistry
University of Pittsburgh
Pittsburgh, Pennsylvania 15260

Dr. Richard Greene
Code 5230
Naval Research Laboratory
Washington, D.C. 20375

Dr. L. Kesmodel
Department of Physics
Indiana University
Bloomington, Indiana 47403

Dr. K. C. Janda
California Institute of Technology
Division of Chemistry and Chemical Engineering
Pasadena, California 91125

Professor E. A. Irene
Department of Chemistry
University of North Carolina
Chapel Hill, Northc Carolina 27514

Dr. Adam Heller
Bell Laboratories
Murray Hill, New Jersey 07974

Dr. Martin Fleischmann
Department of Chemistry
Southampton University
Southampton S09 5NH
Hampshire, England

Dr. John W. Wilkins
Cornell University
Laboratory of Atomic and Solid State Physics
Ithaca, New York 14853

Dr. Richard Smardzewski
Code 6130
Naval Research Laboratory
Washington, D.C. 20375

DL/413/83/01
056/413-2

TECHNICAL REPORT DISTRIBUTION LIST, 056

Dr. R. G. Wallis
Department of Physics
University of California
Irvine, California 92664

Dr. D. Ramaker
Chemistry Department
George Washington University
Washington, D.C. 20052

Dr. P. Hansma
Physics Department
University of California
Santa Barbara, California 93106

Dr. J. C. Hemminger
Chemistry Department
University of California
Irvine, California 92717

Professor T. F. George
Chemistry Department
University of Rochester
Rochester, New York 14627

Dr. G. Rubloff
IBM
Thomas J. Watson Research Center
P.O. Box 218
Yorktown Heights, New York 10598

Professor Horia Metiu
Chemistry Department
University of California
Santa Barbara, California 93106

Captain Lee Myers
AFOSR/NC
Bollig AFB
Washington, D.C. 20332

Professor Roald Hoffmann
Department of Chemistry
Cornell University
Ithaca, New York 14853

Dr. R. W. Plummer
Department of Physics
University of Pennsylvania
Philadelphia, Pennsylvania 19104

Dr. E. Yeager
Department of Chemistry
Case Western Reserve University
Cleveland, Ohio 41106

Professor D. Hercules
University Pittsburgh
Chemistry Department
Pittsburgh, Pennsylvania 15260

Professor N. Winograd
Department of Chemistry
Pennsylvania State University
University Park, Pennsylvania 16802

Dr. G. D. Stein
Mechanical Engineering Department
Northwestern University
Evanston, Illinois 60201

Professor A. Steckl
Department of Electrical and
Systems Engineering
Rensselaer Polytechnic Institute
Troy, NewYork 12181

Professor G. H. Morrison
Department of Chemistry
Cornell University
Ithaca, New York 14853

Dr. David Squire
Army Research Office
P.O. Box 12211
Research Triangle Park, NC 27709

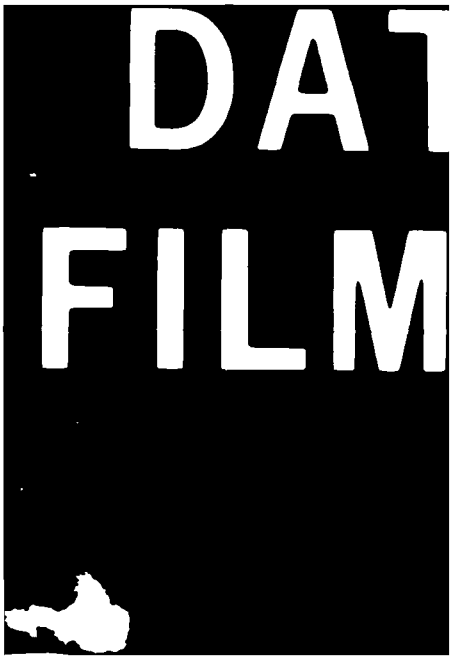
DAT
FILM